Field measurement of wind-driven rain on a low-rise building in the coastal climate of British Columbia

Ge, H., Ph.D., P. Eng.

Krpan, R., P. Eng.

British Columbia Institute of Technology, Burnaby, British Columbia

ABSTRACT

The amount of driving rain received by the building envelope is an important environmental load for building envelope design; however, there is limited information on the rain load to which the building envelope is exposed during its service life. To date, most of the research effort in Canada has focused on assessing the wind-driven rain exposure of a region using historical meteorological data recorded at weather stations rather than wind-driven rain exposure of specific buildings. The actual driving rain load received by building façades is also influenced by the building geometry and design details, for example the size of overhang.

Current best practice guidelines for building envelope wall assemblies lead the user to identify exposure conditions for wind-driven rain in order to select an appropriate type of assembly, especially in the coastal climate of British Columbia (BC). Because of a lack of data, current practice depends on professional judgment. To bridge the knowledge gap, a research program has been designed to instrument an inventory of buildings throughout the lower mainland of BC to collect wind-driven rain data and quantify the influence of building geometry on rain wetting at various locations on the façade.

This paper presents the preliminary results of wind-driven rain measurement on a one-storey low-aspect-ratio building. The on-site wind speed, wind direction, and horizontal rainfall were recorded. The spatial distribution of the wind-driven rain on the east wall was reported. A 130 mm overhang reduced the wetting on the wall surface below it by about two to five times depending on the wind and rain characteristics. The field data will enable the verification and improvement of existing empirical methods and the comparison with Computational Fluid Dynamics models to evaluate the effect of design details.

INTRODUCTION

Wind-driven rain, also referred to as driving rain, is the amount of rainwater that impinges on a vertical wall surface under the influence of wind and is an important environmental condition for building envelope design. It is hard to quantify accurately because of complex interactions between wind and rain and the buildings themselves. Driving rain is affected by the rain and wind characteristics, including rainfall intensity, duration and frequency of rain event, and wind speed and direction. It is also affected by the building characteristics, including topography, building geometry, sheltering provided by surroundings, façade orientation, and location on the façade. Research effort has been made in the past to quantify wind-driven rain by measurements, by empirical correlations, and in recent years, by Computational Fluid Dynamics (CFD) modeling (Blocken, et al, 2002). CFD models provide the flexibility to explore the effects of building geometry, geometric details, and local weather conditions. The model developed by Blocken and Carmeliet (2000) has shown fairly good agreement with measurements. They looked at the

detailed wetting pattern of different building geometry as a function of different wind and rain characteristics (Blocken et al, 2006). The application of numerical models has advanced our understanding of this complex wind-driven rain phenomenon. However, it still remains only practical as a research tool. On the other hand, the empirical methods that correlate the driving rain on building surfaces to meteorological data from weather stations are better suited to design application because of their simplicity and ease of use.

The empirical methods have evolved from a relative measure by assessing the rain exposure of a region to the actual amount of rain that impinges on wall surfaces. Boyd (1963) developed the first 'driving rain map' for Canada using a driving rain index (DRI). The DRI is calculated based on the average annual rainfall and annual mean wind speed, and it is an indication of the wetness of a place. Robinson and Baker (1975) improved the DRI by using hourly wind speed and rainfall data. Fazio et al (1995) made further improvements by considering wall orientation and the co-coincidence of wind and rain. More recently Straube et al (2000) introduced the rain admittance factor (RAF), a factor to transform the wind-driven rain through a free field vertical plane to deposited rain on an actual building. The influence of terrain and topography was also taken into account in their recent work (Straube, 2006) by applying exposure and height factor and topography factor. A detailed procedure is prescribed in the British Standard BS-8104 (1992) to assess wind-driven rain exposure for specific buildings. The procedure includes quantifying the wind-driven rain impinged on a specific wall surface using meteorological data measured at weather stations by introducing four empirical factors: terrain roughness, local topography, obstructions, and building geometry. These empirical methods offer limited guidance with respect to building geometry and design details such as overhang.

To date, there is very limited quantitative information available on the effect of overhangs. Inculet and Surry (1995) studied the influence of building geometry and details including balconies and cornices on the wetting pattern of small-scale models in a boundary layer wind tunnel. Hangan and Surry (2000) investigated the effectiveness of a cornice in reducing rain wetting for a medium-height building using CFD modeling. Both studies found that cornices provide better protection for the area beneath but little influence on the middle zone of the façade. Field surveys in the region of lower mainland BC found a correlation between the building envelope failure occurrence and the size of overhang (MH, 1996). Because of a lack of field data, the current practice in assessing wall exposure conditions for wind-driven rain depends on professional judgment.

To bridge the knowledge gap, an inventory of buildings throughout the lower mainland BC will be instrumented to collect wind-driven rain data. The objective of the research is to verify and improve existing empirical methods in predicting wind-driven rain on wall surfaces of a wide range of building geometry in the coastal climate of BC. The extensive field data will also enable comparison with Computational Fluid Dynamics models to generalize the measurements to evaluate the effect of design details. This paper presents the preliminary results of wind-driven rain measurement on a one-storey low-aspect-ratio building. The effect of wind and rain characteristics on the wetting pattern is also discussed.

MEASUREMENT SETUP

A single-storey building was instrumented with twelve driving rain gauges and measurements were taken over a period of three months from January to April, 2006. Figure 1 illustrates the building and its surrounding environment. It is a low-aspect-ratio structure with mechanical equipment on top of a flat roof. The roof provides a 130 mm overhang. The main body of the building is 43.3 m long, 7.3 m wide and 4.3 m high (Figure 2). The long side is facing east; the

prevailing wind during rain is from this direction. This side wall is exposed to a large parking area and the upstream building is about 150 m away. On its north and west sides are two major roads and the distances to adjacent buildings are about 70 m. On its south side is a row of trees, with the closest tree about 5 m from the building. It is a fairly open site within an urban setting, which makes it a favourable building for a wind-driven rain study.

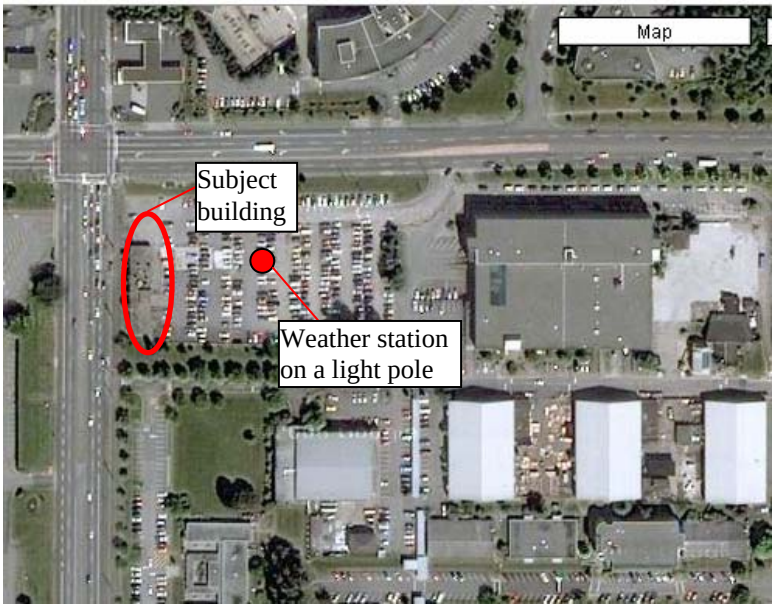

Figure 1: Aerial view of the building site.

Figure 2: East face of the test building

Nine driving rain gauges were installed on the east face of the building and three just around corners for the purpose of monitoring the spatial distribution of wind-driven rain on the façade (Figure 3). The driving rain gauges were made of 5 mm acrylic sheet and have a diamond shape with a dimension of 254 mm by 254 mm. The edge of the collector is 25.4 mm high (Figure 4). The particular shape of the rain gauge allows the effective shedding of runoff rainwater from above. The on-site wind speed and wind direction were measured at 10 m above ground, and the horizontal rain fall was measured at 2 m above ground. The wind sensor and tipping bucket rain gauge were attached to a light pole, which is positioned at a distance of 30 m from the east face of

the building (as shown in Figure 1). The sampling frequency for both wind and rain was 4 minutes. The amount of wind-driven rain was collected by a reservoir and measured manually at the same time every day from January 19 to April 4, 2006.

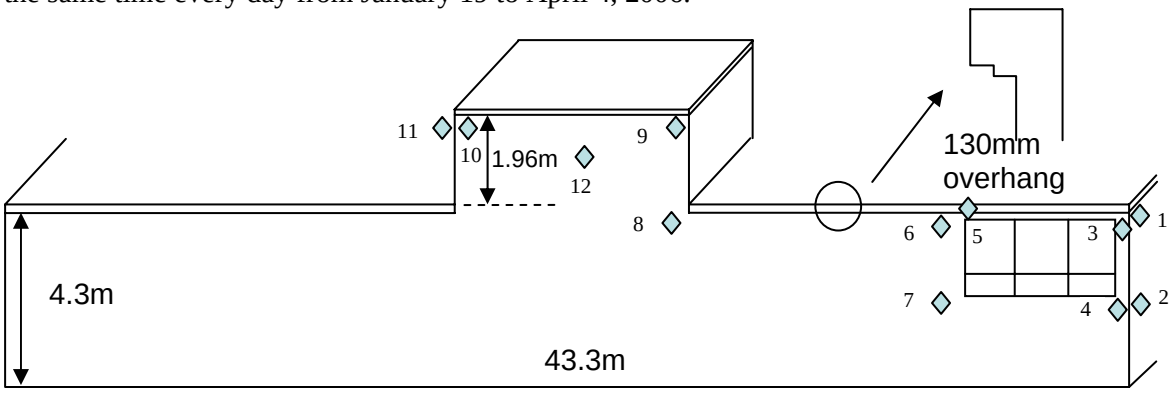

Figure 3. Building geometry and locations of driving rain gauges (not to scale).

Figure 4. Driving rain gauges installed on the east face of the building.

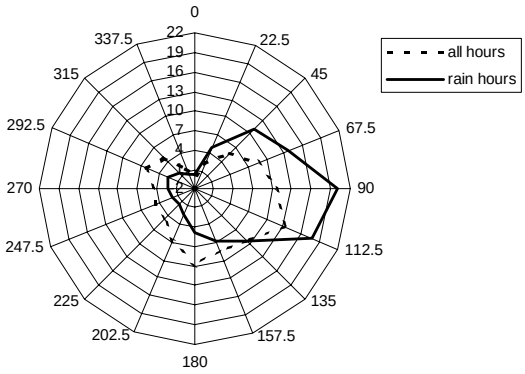

Figure 5. Prevailing wind direction at the building site from January to June, 2006 (in %).

RESULTS

During the measurement period, four main rain events were recorded. The first rain spell was in the winter rainy season from January 19 to February 2. The second spell was in the spring from March 5 to March 10, the third from March 22 to March 27, and the fourth from March 30 to April 4. Figure 5 shows the prevailing wind direction for rainy hours and for all hours. It is clear that the prevailing wind direction at this building site is from the east when it rains. This analysis is based on on-site weather data recorded from January 5 to June 15, 2006.

WIND AND RAIN CORRELATION

The amount of wind-driven rain is largely influenced by wind speed and wind direction. A power law profile is normally used to estimate wind speed at any height for a particular terrain from that measured at 10 m at a meteorological station in open country. For example, ASHRAE (1981) recommends that the wind speed at any height r can be found from:

$$V_r = U_m \kappa r^a \quad (1)$$

Where V_r is the speed at height r meters (m/s), U_m is the wind speed at 10 m above ground recorded at a meteorological station (m/s), and κ and α are constants appropriate for the particular terrain. In an urban environment, ASHRAE recommends κ=0.14, and α=0.40.

The measured on-site wind speed at 10m is compared to that calculated using equation 1 based on the weather data recorded at the Vancouver International airport (Figure 6a). The comparison in wind direction is also made and shown in Figure 6b. Figure 7 shows the comparison for the rain event from March 22 to March 27. The estimated wind speed agrees with measurement in general pattern; however, in some cases the calculation is off by 200%, for example, the peak wind speed values shown in Figure 7a. The on-site wind direction follows the general pattern reported at the airport. It seems that a better agreement is achieved for the rain event from March 5 to March 10 in both wind direction and wind speed than that for the rain event from March 22 to 27.

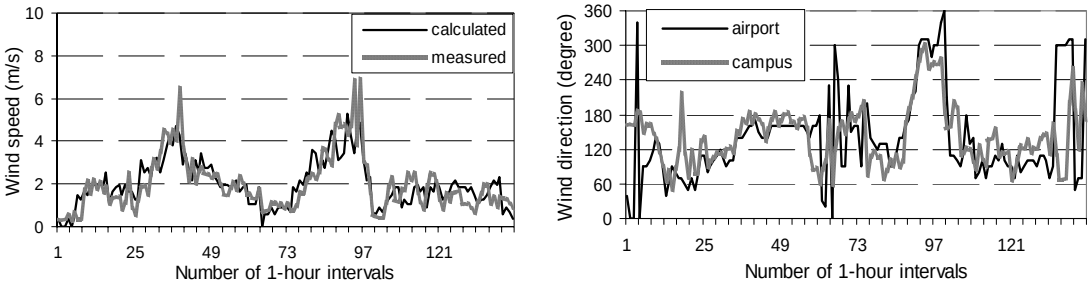

(a) (b)

Figure 6. Rain event from March 5 to March 10. (a) comparison in wind speed between on site measurement and estimation using airport data; (b) comparison in wind direction between on site measurement and that recorded at the airport.

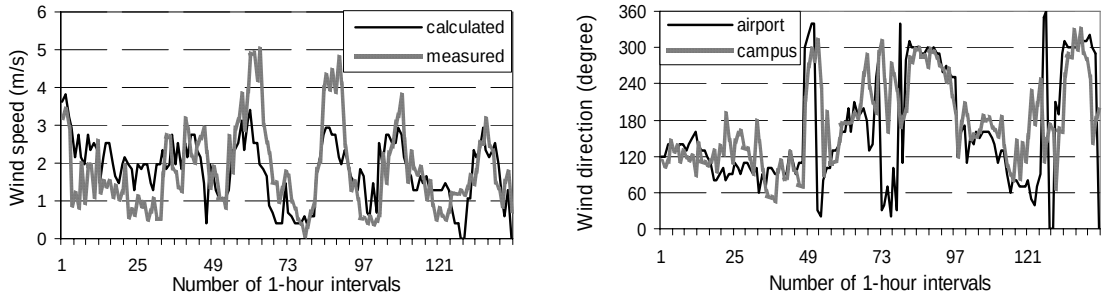

(a) (b)

Figure 7. Rain event from March 22 to March 27. (a) comparison in wind speed between on site measurement and estimation using airport data; (b) comparison in wind direction between on site measurement and that recorded at the airport.

SPATIAL DISTRIBUTION OF WIND-DRIVEN RAIN

The weather data recorded during the rain event from January 19 to February 2 are shown in Figure 8a. The weather data are consolidated from 4-minute intervals to hourly data. The rain intensity is light to moderate, mostly less than 2 mm/hr with a few occasions reaching 4-7 mm/hr. The average wind speed during rain is about 2 m/s and wind direction is at 96^o, almost normal to the building surface. This rain event lasted 15 days with only one day without rain, and when it rained it normally lasted 10-24 hours during this period.

The spatial distribution of wind-driven rain on the façade is indicated by a catch ratio for each monitoring location (Figure 8b). The catch ratio is calculated as the total amount of driving rain collected on the wall surface divided by the total amount of horizontal rainfall over this particular rain event.

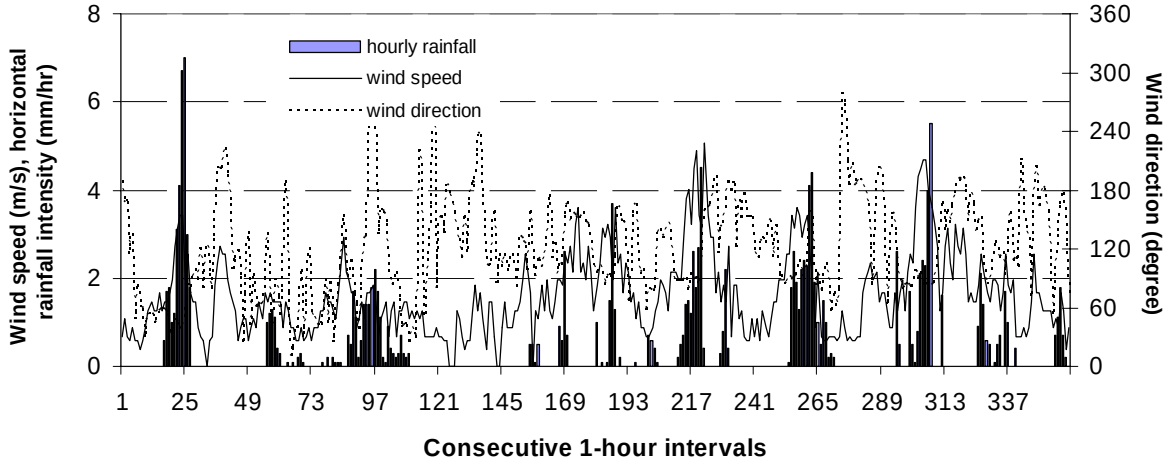

(a)

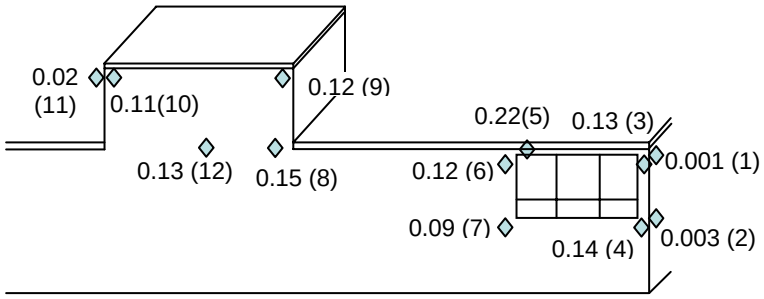

(b)

Figure 8. Measurement results for the rain spell from January 19 to February 2, 2006. (a) hourly horizontal rainfall intensity, wind speed, and wind direction (averaged on a 4-minute basis). Total horizontal rainfall of 130 mm. (b) Spatial distribution of the catch ratio for this rain event (gauge number is shown in brackets).

The results show that the amount of rain deposited on the building surface varies with location. Normally, the top corner receives the highest amount of rain. However, in this case because of the presence of the 130 mm overhang, the amount of rain received at the middle height of the building is almost the same as that at the top corner. There is a loading dock in the middle section of the building, which is about 2 m higher than the lower level. The amount of rain received at the upper corner (gauge no. 9) is almost the same as at the lower corner (gauge no. 3). This indicates that higher levels of the building may not always receive more wind-driven rain. In this case, the 2-metre separation makes little difference. Rain gauge no. 8 was placed at the transition location from the lower part to the loading dock area, where the wind changes direction. This location receives the second largest volume of wind-driven rain. Since during the rain event the prevailing wind direction is from the east, the north corner receives little rain. The south façade receives a smaller quantity as well.

Figure 9 shows the wind-driven rain measurements for the rain event from March 30 to April 2, 2006. In comparison to the first rain event in January, this rain event has a milder wind speed during rain, averaging 1.3 m/s, and a smaller rainfall intensity of less than 1mm/hr. The average wind direction is 127^{o} (south east).

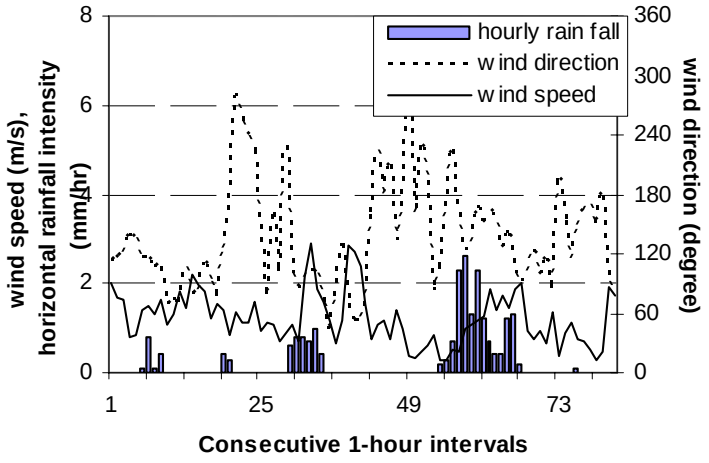

(a)

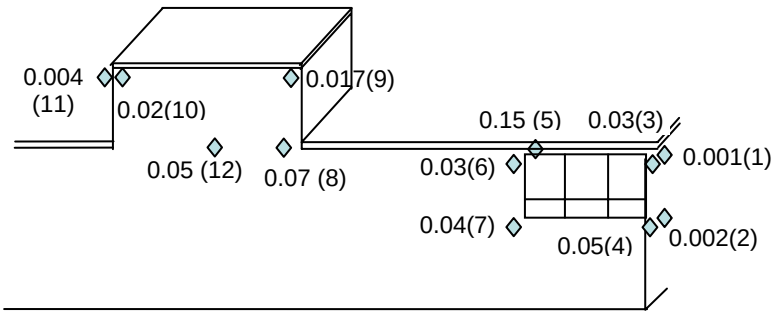

Figure 9. Measurement results for the rain event from March 30 to April 2 2006. (a) hourly horizontal rainfall intensity, wind speed, and wind direction (averaged on a 4-minute basis). Total horizontal rainfall of 21.6 mm. (b) Spatial distribution of the catch ratio for this rain event (gauge number is shown in brackets).

The catch ratio for this particular rain event is smaller than the first rain event for each location although the general distribution pattern is very similar. This is attributed to smaller wind speed and larger wind angle, and potentially to measurement errors. The errors associated with wind-driven rain measurement include adhesion water evaporation, condensation, splashing, and wind error. The error due to adhesion water evaporation is large for light rain (Blocken, 2004). The amount of wind-driven rain impinged on the collection area can only be measured after surface runoff occurs when the accumulated wind-driven rain on the collector exceeds a threshold value. Below this threshold value, the rainwater impinged on the collector surface will evaporate. Above the threshold value, an approximately constant amount of water is adhered to the surface. When rain stops, this amount of adhered water will evaporate. Laboratory testing indicated that the adhesion water for acrylic is approximated as 0.07 mm. For this particular rain event, the error due to adhesion water evaporation is estimated to range from 10% for gauge 5 to 100% for gauge

10. The correction for adhesion water evaporation is accounted for in the calculation of catch ratios. The spatial distribution for these two rain events makes an interesting comparison. To monitor the effect of the 130 mm overhang on reducing the amount of wind-driven rain received by the wall surface underneath, rain gauge no. 5 was placed on the overhang facia and rain gauge no. 6 was placed right beneath the overhang. The rain gauge on the overhang facia receives the largest amount of driving rain, and it is about twice the amount of wind-driven rain received by gauge no. 6 for the first rain event and about five times for the second rain event (Figure 9b). During the first rain event, gauge no. 3 receives almost the same amount as gauge no. 4 (0.13 v.s. 0.14), while during the second rain event gauge no. 3 receives only half of the amount by gauge no. 4. This simple comparison indicates that the effect of overhang on protecting the wall beneath depends on the characteristics of the rain event.

To investigate the potential relationship between the effect of overhang and the characteristics of the rain event, the catch ratios for location 5 and 6 are looked at in greater detail. Figure 10 shows the ratio of the wind-driven rain amount received on location 5 to the wind-driven rain amount received on location 6 as a function of the product of average hourly wind speed, hourly rainfall intensity, and the cosine of the angle between the wind direction and the normal to the wall surface. It seems that with the increase of $UCos(\theta)R_h$, the ratio decreases, so does the rain protection provided by the overhang. However, due to the high complexity of interaction between wind, rain, and the building, any conclusive findings on the quantitative effect of overhang needs to be supported by a large number of accurate field measurements or CFD modeling or wind-tunnel testing. This graph can only be read as an indication that the overhang effect is dependent on the rain and wind characteristics.

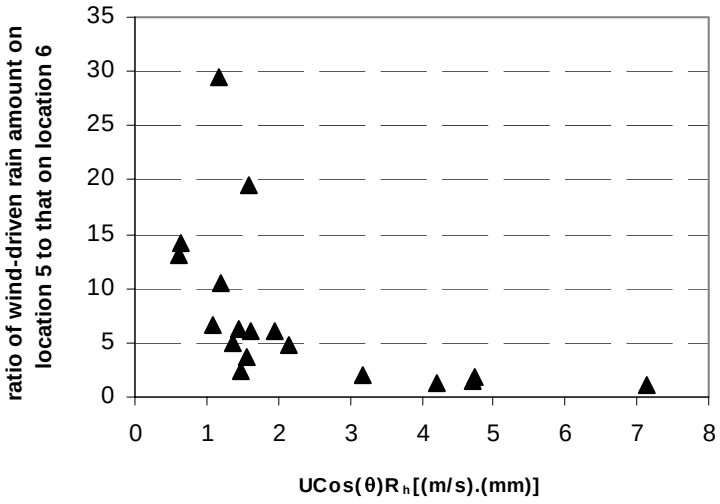

Figure 10. The effect of overhang in reducing wind-driven rain as a function of the rain and wind characteristics. U is the wind speed measured at 10 m above ground (m/s), θ is the angle between wind and the normal to the wall, and R_h is hourly horizontal rainfall (mm).

WALL FACTORS

To generalize measurements on specific buildings, empirical correlations have been developed and used to correlate the weather data recorded from the meteorological station to similar buildings, for example the British standard BS-8104 (1992) prescribed a detailed procedure to assess the wind-driven rain exposure of specific buildings. The procedure includes quantifying

the driving rain that would occur at 10 m above ground level in the middle of an airfield at the geographical location of the proposed wall (equation 3). To take into account the difference in exposure between the "airfield situation" and the "building situation", correction factors are introduced to convert the airfield indices to wall indices. The correction factors include (1) the terrain roughness factor R, (2) the topography factor T, (3) the obstruction factor O, and (4) the wall factor W. Then the amount of wind-driven rain received by a specific location on a specific wall is predicted to be:

$$R_{wdr}=R_{airfield}\cdot R\cdot T\cdot O\cdot W \tag{2}$$

$$R_{airfield}=\frac{2}{9}\cdot U\cdot R_h^{8/9}\cos(\theta-90^o) \tag{3}$$

U is the wind speed in m/s, R_h is the horizontal rainfall in mm/hr, and θ is the wind direction.

The terrain roughness factor takes into account the variability of the mean wind speed at the site due to the height above the ground and the upstream roughness of the terrain. The topography factor accounts for the increase of the mean wind speed over isolated hills and escarpments. The obstruction factor takes into account the shelter by the nearest obstacle of similar dimensions to the wall. The wall factor is assumed to take into account the variation of wind-driven rain over the surface of the wall. The British standard provides simplified wall factors for a limited number of building geometries, typically low-rise buildings. These wall factors were generated based on field measurements. However, the current standard does not provide wall factors for corners and edges, neither covers details such as different size of overhang.

The procedure prescribed by the British Standard is followed to generate wall factors for the test building. Once the wall factors are defined, they can be used to estimate wind-driven rain on a similar building at different locations. In this particular case, weather data were measured on site; therefore, the terrain roughness factor R=1, the upstream side of the building is an open area without obstruction, so T=1 and O=1. Therefore, the wall factor W is equal to the ratio of driving rain measured on the wall (R_{wdr}) to the quantity passing through an equivalent unobstructed air space ($R_{airfield}$). The wall factors for each rain event are calculated and listed in Table 1. The results show that the wall factors for the same location vary with rain event. It seems that the location underneath the overhang is more significantly influenced by the wind and rain characteristics. For example, wall factors for locations 3, 6, 9, and 10, which are directly underneath the 130 mm overhang, are much smaller for the 3rd and 4th rain event compared to rain events 1 and 2. For other locations such as 4, 7, and 12 at the mid-height of the wall, the variations are smaller. The wall factors for location 5 (on the overhang facia) and location 8 (geometry transition) vary only slightly with rain events.

Table 1. Wall factors calculated for locations on the east façade for four rain events

Rain event	total rainfall (mm)	wind speed (m/s)	wind direction	Wall factor at different locations								
				3	4	5	6	7	8	9	10	12
I	130	2.3	96	0.24	0.27	0.41	0.22	0.18	0.27	0.23	0.21	0.25
II	59.6	2.4	114	0.28	0.29	0.41	0.24	0.21	0.30	0.24	0.22	0.25
III	39.6	1.5	113	0.08	0.19	0.44	0.08	0.16	0.23	0.04	0.04	0.17
IV	21.6	1.3	127	0.07	0.16	0.54	0.06	0.12	0.21	0.03	0.04	0.15
Total				0.26	0.30	0.48	0.23	0.20	0.31	0.23	0.21	0.27

The results show that the wall factor is not a constant value, which means the spatial distribution of wind-driven rain changes with each rain event. Previous studies (Inculet et al, 1995; Blocken and Cameliet, 2006) showed that the wind angle approaching the façade is a significant factor influencing the amount of driving rain impinged on a particular location of the wall. Figure 11 plots wall factor variation against wind direction for locations 3 and 10, the wall factors are calculated using daily data. The general trend is that the wall factor decreases when the wind is approaching from an angle away from the normal to the wall surface. As discussed earlier, wind speed and rainfall intensity also have a significant impact on the amount of driving rain. The wide range of wall factors measured when wind blows from the east (normal to the wall surface) is attributed to the variation of wind speed and rainfall intensity. The wall factor for each location on the east façade is also calculated using the total rainfall over the four rain events and is shown in Figure 12.

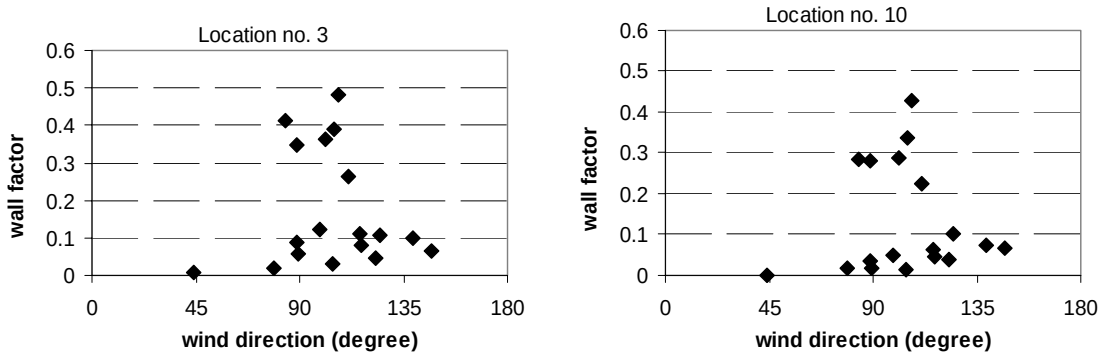

Figure 11. Wall factor variations against wind direction for selected locations on east wall.

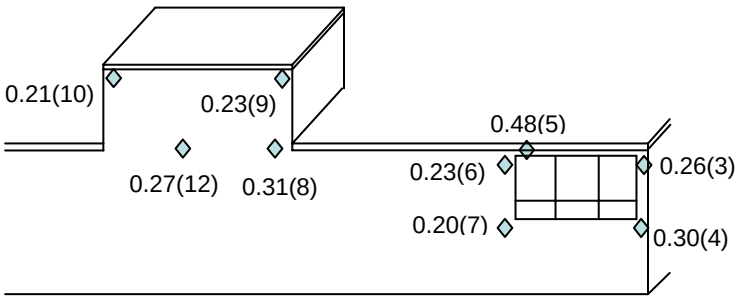

Figure 12. Wall factors on the east wall surface (gauge number is in the brackets).

CONCLUSIONS

Wind-driven rain measurements were conducted on a single-storey low-aspect-ratio building in the coastal climate of British Columbia. This paper reports the spatial distribution of wind-driven rain on the east façade of the test building using catch ratio and wall factors as indicators. The wall factors were generated using measured data by following the procedure prescribed in the British Standard 8104. The preliminary results show that corners and edges receive the largest amount of rain. The 130 mm overhang reduced the amount of rain received by the wall surface

underneath; however, its effectiveness depends on the wind and rain characteristics. The wall factor, which accounts for spatial variation, is not a constant and varies with rain event. More data will be collected and analyzed in order to draw more conclusive findings. The field data will be used to verify and improve existing empirical methods to predict wind-driven rain on wall surfaces.

ACKNOWLEDGEMENT

The authors would like to acknowledge the contributions by Blue Lee, Takashi Sawada, Eddie Chen, Kevin Kinrade, Jeremias Souza, Todd Loucks, and Monica Lp. These students helped collect the wind-driven rain data.

REFERENCES

1. ASHRAE (1981). Handbook of fundamentals, New York.
2. Blocken, B. and Carmeliet, J. (2006). On the validity of the cosine projection in wind-driven-rain calculations on buildings. Building and Environment. Vol. 41 (9), pp. 1182-1189.
3. Blocken, B. (2004). Wind-driven rain on buildings: measurements, numerical modeling, and application. Doctoral Thesis, Katholieke Universiteit Leuven, Belgium.
4. Blocken, B., H. Hens, and J. Carmeliet (2002). Methods for quantification of driving rain on buildings. ASHRAE Transactions, Vol. 109, pp. 338-350.
5. Blocken, B. and Carmeliet J. (2000). Driving rain on building envelopes - I: numerical estimation and full-scale experimental verification. Journal of Thermal Envelope and Building Science 24(1): 61-85.
6. Boyd, D.W. (1963). Driving-Rain Map of Canada. DBR/National Research Council, TN 398, Ottawa.
7. BSI. (1992). BS8104: Code of practice for assessing exposure of walls to wind-driven rain. British Standard Institution.
8. Fazio, P., Mallidi, S.R. and Zhu, D. (1995). A quantitative study for the measurement of driving rain exposure in Montreal region. Building and Environment, Vol. 30, No. 1, pp. 1-11.
9. Inculet, D. and Surry, D. (1995). Simulation of wind driven rain and wetting patterns on buildings. Research report for Canadian Mortgage and Housing Corporation, Ottawa.
10. Morrison Hershfield, (1996). Survey of building envelope failures in the coastal climate of British Columbia. Research report for Canadian Mortgage and Housing Corporation, Ottawa.
11. Robinson G. and M.C. Baker (1975). Wind-driven rain and buildings. Technical paper No. 445. Division of Building Research, National Research Council of Canada, Ottawa.
12. Straube (2006). Driving rain loads for Canadian building design. Research report for Canadian Mortgage and Housing Corporation, Ottawa.
13. Straube, J. and Burnett, E. (2000). Pressure moderation and rain control for multi-wythe masonry walls. Proceedings of the International Building Physics Conference, Eindhoven University of Technology, Einhoven, the Netherlands, pp. 179-186.
14. Hangan H., and Surry, D. (2000). Wind-driven rain study for Governor's road project, Dundas, Ontario. Research report for Canadian Mortgage and Housing Corporation, Ottawa.